Editors' Suggestion Featured in Physics

Quantum Key Distribution over 658 km Fiber with Distributed Vibration Sensing

Jiu-Peng Chen,[1,2,3] Chi Zhang,[1,2,3] Yang Liu,[3,*] Cong Jiang,[3] Dong-Feng Zhao,[1] Wei-Jun Zhang,[4] Fa-Xi Chen,[3] Hao Li,[4] Li-Xing You,[4] Zhen Wang,[4] Yang Chen,[1] Xiang-Bin Wang,[2,3,5] Qiang Zhang,[1,2,3,†] and Jian-Wei Pan[1,2,‡]

[1]*Hefei National Laboratory for Physical Sciences at Microscale and Department of Modern Physics, University of Science and Technology of China, Hefei 230026, China*

[2]*CAS Center for Excellence and Synergetic Innovation Center in Quantum Information and Quantum Physics, University of Science and Technology of China, Hefei 230026, China*

[3]*Jinan Institute of Quantum Technology, Jinan, Shandong 250101, China*

[4]*State Key Laboratory of Functional Materials for Informatics, Shanghai Institute of Microsystem and Information Technology, Chinese Academy of Sciences, Shanghai 200050, China*

[5]*State Key Laboratory of Low Dimensional Quantum Physics, Department of Physics, Tsinghua University, Beijing 100084, China*

(Received 22 October 2021; accepted 29 March 2022; published 2 May 2022)

Twin-field quantum key distribution (TFQKD) promises ultralong secure key distribution which surpasses the rate distance limit and can reduce the number of the trusted nodes in long-haul quantum network. Tremendous efforts have been made toward implementation of TFQKD, among which, the secure key with finite size analysis can distribute more than 500 km in the lab and in the field. Here, we demonstrate the sending-or-not-sending TFQKD experimentally, achieving a secure key distribution with finite size analysis over a 658 km ultra-low-loss optical fiber. Meanwhile, in a TFQKD system, any phase fluctuation due to temperature variation and ambient variation during the channel must be recorded and compensated, and all this phase information can then be utilized to sense the channel vibration perturbations. With our quantum key distribution system, we recovered the external vibrational perturbations generated by artificial vibroseis on both the quantum and frequency calibration link, and successfully located the perturbation position in the frequency calibration fiber with a resolution better than 1 km. Our results not only set a new distance record of quantum key distribution, but also demonstrate that the redundant information of TFQKD can be used for remote sensing of the channel vibration, which can find applications in earthquake detection and landslide monitoring besides secure communication.

DOI: 10.1103/PhysRevLett.128.180502

Introduction.—Quantum key distribution (QKD) [1–6] offers the theoretical provable way to distribute secure keys. However, the channel loss is an inevitable barrier for long distance QKD since a quantum signal cannot be amplified. For a transmission η, the theoretical upper bound of the secure key rate is limited to 1.44η, known as the Pirandola-Laurenza-Ottaviani-Bianchi (PLOB) bound [7]. This upper bound is valid for all the repeaterless QKD protocols which include the commonly decoy-state based BB84 [8–10], and the measurement-device-independent QKD [11,12] which closes all security loopholes of measurement devices. Without the practical quantum repeater, an intermediate solution to achieve the long haul QKD network is to set several trusted relay nodes. Although the trusted relay networks are successfully demonstrated in the field [13], the increased number of trusted relays might increase the security risk and raise the cost.

Different from the traditional QKD protocols, the twin-field QKD (TFQKD) [14] improves the secure key rate scaling to $\sqrt{\eta}$ without using quantum memory. This may provide a solution to reach a longer distance and to reduce the number of trusted relays. Recently, the feasibility of distributing secure keys over a long distance is proved experimentally [15–23]. Notably, with full security analysis considering the finite size effect, an experimental demonstration of sending or not sending TFQKD (SNS TFQKD) [24] is realized with a record long distance of more than 500 km in the lab [19,22] and in the field [23]. In order to achieve a secure final key, one needs to overcome the challenging problem finite key effects with a relatively small data size. In the case of not considering the data finite size, one can even obtain a positive key rate at a distance of 600 km [22].

Realizing TFQKD is challenging, because the protocols require phase sensitive single-photon interference. Any phase differences, caused by laser wavelength differences or channel fiber vibration, may reduce the interference visibility. Techniques such as time-frequency metrology [17,19,23] and optical phase locking loop [15,16,22] have been developed to eliminate the wavelength difference; real-time [16,22] or postprocessing [17,19–21,23] compensation have been developed to eliminate the fast fiber vibration.

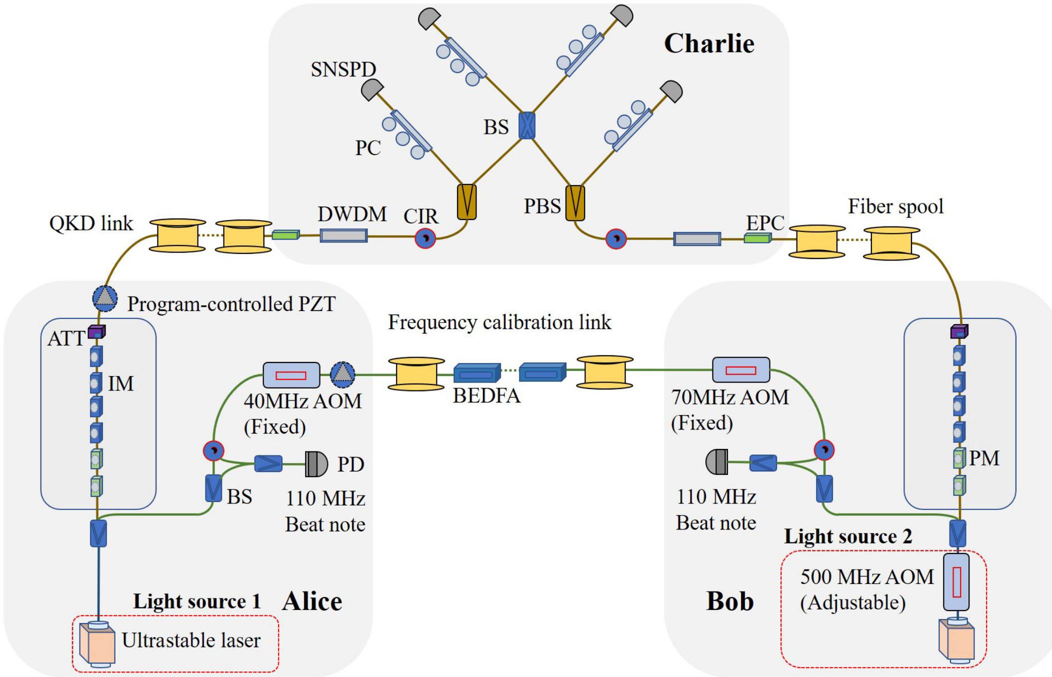

FIG. 1. Schematic of experimental setup. In Alice's (Bob's) lab, a seed laser is locked to an ultra-low-expansion (ULE) glass cavity to achieve a subhertz linewidth by using the Pound-Drever-Hall (PDH) [41,42] technique. After PDH locking, a 500 MHz acoustic-optic modulator (AOM) with adjustable carrier frequency is inserted at Bob to eliminate the frequency difference of the two stable lasers. Then, the ultrastable light sources are split into two parts, respectively; one is used for QKD, the other is sent to the other user via a 500 km frequency calibration fiber link for heterodyne interference. Bidirectional erbium-doped fiber amplifiers (BEDFAs) are inserted every 50 km to maintain the power of the transmitted light, two AOMs with fixed carrier frequency of 40 and 70 MHz are inserted at both ends of the link to filter the reflection in the channel. PD: photodiode. In the QKD part, the light is modulated with phase modulators (PMs) and intensity modulators (IMs) and attenuated to a single photon level with an attenuator (ATT), to generate the quantum signals with the phase reference signals. The light is finally sent to Charlie via 329.3 and 329.4 km ultra-low-loss fiber spools (658.7 km) for detection. Charlie uses a dense wavelength division multiplexer (DWDM), a circulator (CIR) to filter the noises before the polarization beam splitter (PBS) and the beam splitter (BS). The interference results are detected by superconducting nanowire single-photon detectors (SNSPDs). Additionally, the fiber stretchers are inserted into the QKD channel and the wavelength calibration channel, as the artificial vibroseis. EPC: electric polarization controller; PC: polarization controller.

Besides supporting TFQKD, the obtained information in fast phase compensation actually reflects the real-time phase variation of the transmitted light in the optical fiber. This information can also be utilized to detect the vibrational perturbation in the channel. As such, the redundant information obtained in an installed TFQKD system might be used as a fiber-optic sensor to detect critical vibrations in the channel. Different from the well-known distributed acoustic fiber sensing [25–27] technique, the phase-tracking method used in TFQKD analyzes the transmitted light, not the backscattered light. This technique is similar to the phase-based frequency metrology interferometric technique [28–33], making it possible to achieve an ultra-long vibrational sensing length. With this interferometric method, the measured phase signal will be the result of integration of perturbations along the whole fiber. Fortunately, by using the simultaneous bidirectional phase tracking [33], it is possible to identify the perturbation location by cross-correlating the time difference between the signals of Alice and Bob.

Here, we demonstrated SNS TFQKD [24] experimentally through a 658 km ultra-low-loss optical fiber with a total loss of 106 dB. The secure key rate is 9.22×10^{-10} per pulse after collecting 27.8 h data for considering the finite key size effect in security analysis. Meanwhile, we insert an artificially vibroseis in the channel to generate specific vibration signals. With the same TFQKD experimental setup, we recovered the vibration signals generated by the vibroseis. Further, by cross-correlating the vibrational signals at the two users, we successfully located the vibroseis to a 1 km precision over the 500 km frequency locking fibers, which is, as far as we know the longest reported distance [33,34].

The experimental setup is shown in Fig. 1. Alice and Bob use two independent ultrastable lasers of which the relative frequency difference is eliminated. The light is modulated to a pattern that the single-photon-level quantum signal pulses are time multiplexed with strong phase reference pulses. The signals from Alice and Bob are sent to Charlie through 329.3 and 329.4 km (658.7 km in total) ultra-low-loss fiber spools with a transmission of 52.9 and 53.1 dB (106 dB in total). After interference at Charlie's beam splitter (BS), the signals are detected by two superconducting nanowire single photon detectors (SNSPDs), and recorded by a time tagger. (See Supplemental Material [35–40] for details of the experimental setup).

The key to realize SNS TFQKD is the stable single photon interference, which requires that Alice's and Bob's lasers are locked to the same frequency. We solve this problem by adapting the frequency metrology technology. First, the linewidth of Alice's (Bob's) seed laser is suppressed to subhertz by locking to an ultra-low-expansion (ULE) glass cavity using the Pound-Drever-Hall (PDH) technique [41,42]. After PDH locking, the relative frequency difference drift rate is smaller than 0.1 Hz/s. Then a 500 MHz acoustic-optic modulator (AOM) with adjustable carrier frequency is inserted at Bob for feedback. In order to obtain the cumulative frequency difference, the light is sent to the other user through 500 km fiber spools for heterodyne detection. To eliminate the noise due to back-reflected Rayleigh scattering or imperfect connections, two AOMs with 40 and 70 MHz fixed carrier frequencies are inserted at Alice and Bob, respectively, to shift the frequency of the transmitted laser in a different direction. Then an electronic filter is used to eliminate the noise due to channel reflection. The cumulative frequency difference introduced in the channel is calibrated and compensated every hour, by adjusting the carrier frequency of the 500 MHz AOM based on the heterodyne detection result.

To achieve single photon interference, the relative phase between Alice and Bob should also be compensated. This is achieved by phase estimation with strong pulses. The fast phase fluctuation is mainly contributed by the accumulation of mechanical perturbations such as vibration and sound through the long fiber channel. Now that the phase fluctuation can be compensated in TFQKD, the phase perturbations induced by vibration through the channel can be derived straightforwardly. In other words, we can regard the TFQKD system as a sensing equipment to detect vibrations in the channel.

Besides the quantum channel, the frequency calibration link can also be used to detect vibration. Similar to that in the QKD link, the phase of the radio frequency (rf) signal measured in the heterodyne detection carry the perturbation information of the fiber vibration. In the QKD link, a single detection is performed and only the global phase in the fiber can be extracted. In the frequency calibration link, with simultaneous measuring the phase change at Alice and Bob, the relative delay of the vibration event can be also obtained with cross-correlating method. The position of the vibroseis can be easily calculated with this relative delay and the total length of the channel.

To investigate the vibration perturbations, we inserted program-controlled piezoelectric ceramic transducer (PZT) vibration generators in the quantum channel and frequency calibration channel, as shown in Fig. 1. (See Supplemental Material [35–40] for details of the vibration test methods).

In the experiment, we first explore the longest possible TFQKD distribution distance with our setup. A 658 km G.652 ultra-low-loss fiber with a total loss of 106 dB is used as the quantum channel, which is 0.161 dB/km on average, including the connections. The component loss is optimized to 1.3 dB in Charlie. Then, we adopted high performance SNSPDs with a detection efficiency of 82% and an effective dark count rate of 4 Hz to detect the interference, and set a time gate of 0.3 ns to suppress noise. The final noise is optimized to be 6×10^{-9} per pulse, about 80% of which is from re-Rayleigh scattering [19].

In about 27.8 h, a total of 1.007×10^{13} signals are sent at the 100 MHz effective system frequency, yielding 5.28×10^{6} valid detections. We observe a quantum phase flip error rate in X basis of around 5%, with a base-line error rate of around 2.8%. The bit-flip error rate in Z basis is 26.29% before actively odd parity pairing (AOPP) [43–45] and decreases to 2.12% after AOPP, while the phase error rate increases to 13.36%.

The secure key rate is then calculated following Eq. (1), considering the finite data size effect [43,46]:

$$R = \frac{1}{N_t}\left\{ n_1'[1 - H(e_1^{ph})] - f n_t' H(E_Z) - 2\log_2 \frac{2}{\varepsilon_{cor}} - 4 \log \frac{1}{\sqrt{2}\varepsilon_{PA}\hat{\varepsilon}} \right\}, \tag{1}$$

where R is the final key rate, n_1', e_1^{ph}, n_t', and E_Z are the number of untagged-bits, the phase-flip error rate, the number of survived bits, and the bit-flip error rate of untagged-bits after AOPP. $f = 1.16$ is the error correction efficiency. N_t is the total number of signal pulses, $\varepsilon_{cor} = 1 \times 10^{-10}$ and $\varepsilon_{PA} = 1 \times 10^{-10}$ are the failure probability of error correction process and privacy amplification process, $\hat{\varepsilon} = 1 \times 10^{-10}$ is the coefficient of the chain rules of smooth min entropy and max entropy.

The final secure key rate is $R = 9.22 \times 10^{-10}$, which is about 0.092 bit per second considering 100 MHz effective system frequency. We summarize our theoretical simulation and experimental result in Fig. 2. The obtained secure key rate here is more than one order of magnitude higher than the absolute PLOB bound. (See Supplemental Material [35–40] for details of experimental parameters and results).

Next, we modulate the PZT vibration generators with fixed frequencies to simulate the vibration perturbations in the channel. In the case the PZT vibration takes place in the 658 km quantum channel, the phase drift is recovered by

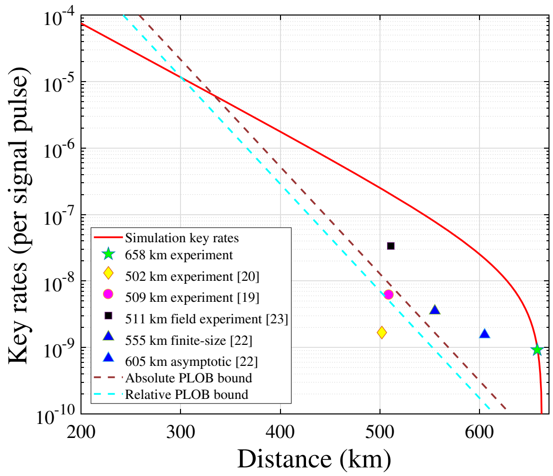

FIG. 2. Secure key rates of the SNS TFQKD experiment. The green star indicates the experimental result over 658 km ultra-low-loss optical fibers, with the secure key rate of $R = 9.22 \times 10^{-10}$. The yellow diamond, purple circle, and blue triangle indicate the experimental results of Refs. [19,20,22] in the lab. The black square indicates the experimental result of Ref. [23] in field. The red curve is the simulation result with the experimental parameters. The brown dotted line and cyan dotted line show the absolute and relative PLOB bound [7].

consequently calculating the relative phase difference with the phase reference pulses. We set the modulation to sinusoidal signal with selected frequencies of 1, 10, 100, and 1000 Hz, respectively, which is the frequency range of interest in seismic and acoustic wave sensing. The recovered phase variation perfectly matches the active modulation signal, i.e., the externally applied vibration on the fiber as shown in Fig. 3. The phase change induced ranges from 1 to 75 radians due to the different frequency responses of our vibration source. As a comparison, the phase changes caused by the seismic waves is in the range of several hundred to several thousand radians [33]. (See Supplemental Material [35–40] for details of the frequency responses).

In the case the PZT vibration takes place in the frequency calibration channel, we set the channel length to nominal 0, 200, and 500 km, respectively, and install the vibroseis at Alice with different vibration frequencies. Here, the vibration signal is recovered by electronically decoding phase perturbations of the rf signal of heterodyne. As shown in Fig. 4, the recovered phase variation shows a frequency and waveform exactly the same as that of the driving signal in all the fiber lengths. The vibroseis position is measured by calculating the relative time delay of the vibration signals at Alice and Bob. For the case of a fiber length of 500 km and the vibroseis installed at Alice as an example, the relative time delay between the Alice and Bob's signals is measured as 2.513 ms by cross-correlation. By adopting the speed of light in the fiber to be 2.0×10^8 m/s, this yields a location of the vibration source at 502.6 km away from Bob. Similarly, the vibroseis is located to 200.0 km away from Bob, with the relative delay to be 1.000 ms, for the 200 km case. The precision of location is better than 1 km, which is mainly limited by the sampling rate of our phase measurement. We note that in general, vibrations from different sources have different characteristics. In principle, the location of each vibration site can be determined with the advanced signal processing method, including time-gated cross-correlation calculations with appropriate filtering (see Supplemental Material [35–40] for discussion of multipoint sensing).

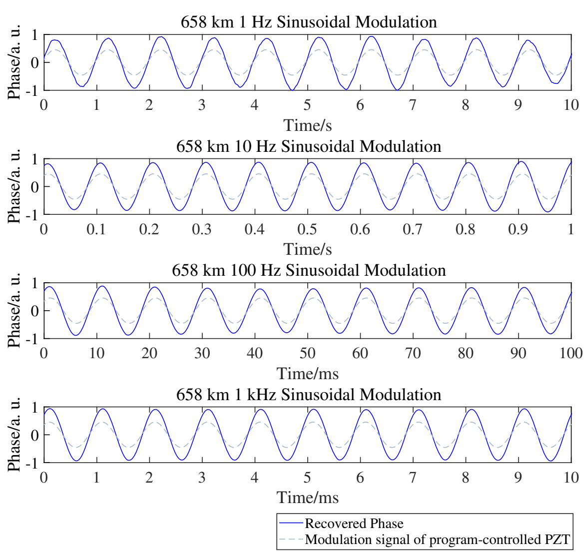

FIG. 3. Vibration test results via the QKD link. The blue curve indicates the recovered relative phase variation signal. The gray dotted line indicates the modulation signal of program-controlled PZT.

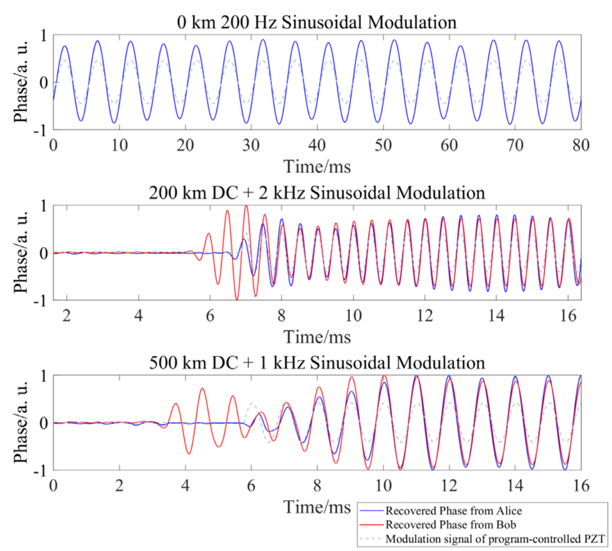

FIG. 4. Vibration test results via frequency calibration link. The blue curve and red curve indicate the recovered phase variation signals of Alice and Bob. The gray dotted line indicates the modulation signal of program-controlled PZT.

In conclusion, we demonstrated SNS TFQKD over 658 km ultra-low-loss optical fiber spools experimentally, achieving a secure key rate of 9.22×10^{-10} per pulse with the finite key size effect considered. Compared with the satellite based QKD system that is able to distribute secure keys over 1120 km [47], much longer than our system; the TFQKD system can work full time and is robust to environment changes such as bad weather or in daytime. We recover 1 Hz–1 kHz vibration perturbations on the fiber with the phase reference and the frequency locking channel, and locate the vibroseis with a precision better than 1 km over the 500 km fiber spools. Our Letter provides a proof of principle that the TFQKD architecture is able to be used for ultralong distance vibration sensing, while distributing secure keys. The next step will be sensing vibrations with the TFQKD system in the field, where the length of the calibration link is the same as the quantum link [23]. We expect that the developed techniques may expand the application of QKD networks, specifically in the field of earthquake detection, landslide monitoring and highway traffic monitoring, etc, where a distributed seismic detection is necessary.

This work was supported by the National Key R&D Program of China (Grants No. 2017YFA0303900, No. 2017YFA0304000, No. 2020YFA0309800), the National Natural Science Foundation of China (T2125010), the Chinese Academy of Sciences (CAS), Key R&D Plan of Shandong Province (Grants No. 2019JZZY010205, No. 2020CXGC010105), and Anhui Initiative in Quantum Information Technologies.

J.-P. C. and C. Z. contributed equally.

*liuyang@jiqt.org
†qiangzh@ustc.edu.cn
‡pan@ustc.edu.cn

[1] C. Harles H. Bennett and Gilles Brassard, Quantum cryptography, in *Proceedings of the IEEE International Conference on Computers, Systems, and Signal Processing, Bangalore, India,* (1984), pp. 175–179.

[2] Nicolas Gisin, Grégoire Ribordy, Wolfgang Tittel, and Hugo Zbinden, Quantum cryptography, Rev. Mod. Phys. **74**, 145 (2002).

[3] Nicolas Gisin and Rob Thew, Quantum communication, Nat. Photonics **1**, 165 (2007).

[4] Valerio Scarani, Helle Bechmann-Pasquinucci, Nicolas J Cerf, Miloslav Dušek, Norbert Lütkenhaus, and Momtchil Peev, The security of practical quantum key distribution, Rev. Mod. Phys. **81**, 1301 (2009).

[5] Feihu Xu, Xiongfeng Ma, Qiang Zhang, Hoi-Kwong Lo, and Jian-Wei Pan, Secure quantum key distribution with realistic devices, Rev. Mod. Phys. **92**, 025002 (2020).

[6] Stefano Pirandola, Ulrik L Andersen, Leonardo Banchi, Mario Berta, Darius Bunandar, Roger Colbeck, Dirk Englund, Tobias Gehring, Cosmo Lupo, Carlo Ottaviani *et al.*, Advances in quantum cryptography, Adv. Opt. Photonics **12**, 1012 (2020).

[7] Stefano Pirandola, Riccardo Laurenza, Carlo Ottaviani, and Leonardo Banchi, Fundamental limits of repeaterless quantum communications, Nat. Commun. **8**, 15043 (2017).

[8] Won-Young Hwang, Quantum Key Distribution with High Loss: Toward Global Secure Communication, Phys. Rev. Lett. **91**, 057901 (2003).

[9] Xiang-Bin Wang, Beating the Photon-Number-Splitting Attack in Practical Quantum Cryptography, Phys. Rev. Lett. **94**, 230503 (2005).

[10] Hoi-Kwong Lo, Xiongfeng Ma, and Kai Chen, Decoy State Quantum Key Distribution, Phys. Rev. Lett. **94**, 230504 (2005).

[11] Hoi-Kwong Lo, Marcos Curty, and Bing Qi, Measurement-Device-Independent Quantum Key Distribution, Phys. Rev. Lett. **108**, 130503 (2012).

[12] Samuel L Braunstein and Stefano Pirandola, Side-Channel-Free Quantum Key Distribution, Phys. Rev. Lett. **108**, 130502 (2012).

[13] Yu-Ao Chen *et al.*, An integrated space-to-ground quantum communication network over 4,600 kilometres, Nature (London) **589**, 214 (2021).

[14] Marco Lucamarini, Zhiliang L. Yuan, James F. Dynes, and Andrew J. Shields, Overcoming the rate-distance limit of quantum key distribution without quantum repeaters, Nature (London) **557**, 400 (2018).

[15] M. Minder, M. Pittaluga, G. L. Roberts, M. Lucamarini, J. F. Dynes, Z. L. Yuan, and A. J. Shields, Experimental quantum key distribution beyond the repeaterless secret key capacity, Nat. Photonics **13**, 334 (2019).

[16] Shuang Wang, De-Yong He, Zhen-Qiang Yin, Feng-Yu Lu, Chao-Han Cui, Wei Chen, Zheng Zhou, Guang-Can Guo, and Zheng-Fu Han, Beating the Fundamental Rate-Distance Limit in a Proof-of-Principle Quantum Key Distribution System, Phys. Rev. X **9**, 021046 (2019).

[17] Yang Liu, Zong-Wen Yu, Weijun Zhang, Jian-Yu Guan, Jiu-Peng Chen, Chi Zhang, Xiao-Long Hu, Hao Li, Cong Jiang, Jin Lin *et al.*, Experimental Twin-Field Quantum Key Distribution through Sending or Not Sending, Phys. Rev. Lett. **123**, 100505 (2019).

[18] Xiaoqing Zhong, Jianyong Hu, Marcos Curty, Li Qian, and Hoi-Kwong Lo, Proof-of-Principle Experimental Demonstration of Twin-Field Type Quantum Key Distribution, Phys. Rev. Lett. **123**, 100506 (2019).

[19] Jiu-Peng Chen, Chi Zhang, Yang Liu, Cong Jiang, Weijun Zhang, Xiao-Long Hu, Jian-Yu Guan, Zong-Wen Yu, Hai Xu, Jin Lin *et al.*, Sending-or-Not-Sending with Independent Lasers: Secure Twin-Field Quantum Key Distribution over 509 km, Phys. Rev. Lett. **124**, 070501 (2020).

[20] Xiao-Tian Fang, Pei Zeng, Hui Liu, Mi Zou, Weijie Wu, Yan-Lin Tang, Ying-Jie Sheng, Yao Xiang, Weijun Zhang, Hao Li *et al.*, Implementation of quantum key distribution surpassing the linear rate-transmittance bound, Nat. Photonics **14**, 422 (2020).

[21] Hui Liu, Cong Jiang, Hao-Tao Zhu, Mi Zou, Zong-Wen Yu, Xiao-Long Hu, Hai Xu, Shizhao Ma, Zhiyong Han, Jiu-Peng Chen *et al.*, Field Test of Twin-Field Quantum Key Distribution through Sending-or-Not-Sending over 428 km, Phys. Rev. Lett. **126**, 250502 (2021).

[22] Mirko Pittaluga, Mariella Minder, Marco Lucamarini, Mirko Sanzaro, Robert I Woodward, Ming-Jun Li, Zhiliang Yuan, and Andrew J Shields, 600 km repeater-like quantum communications with dual-band stabilisation, Nat. Photonics **15**, 530 (2021).

[23] Jiu-Peng Chen, Chi Zhang, Yang Liu, Cong Jiang, Wei-Jun Zhang, Zhi-Yong Han, Shi-Zhao Ma, Xiao-Long Hu, Yu-Huai Li, Hui Liu *et al.*, Twin-field quantum key distribution over a 511 km optical fibre linking two distant metropolitan areas, Nat. Photonics **15**, 570 (2021).

[24] Xiang-Bin Wang, Zong-Wen Yu, and Xiao-Long Hu, Twin-field quantum key distribution with large misalignment error, Phys. Rev. A **98**, 062323 (2018).

[25] J. Mestayer, Barbara Cox, P. Wills, D. Kiyashchenko, J. Lopez, M. Costello, S. Bourne, G. Ugueto, R. Lupton, G. Solano *et al.*, Field trials of distributed acoustic sensing for geophysical monitoring, in *SEG technical program expanded abstracts 2011* (Society of Exploration Geophysicists, San Antonio, Texas, 2011), pp. 4253–4257.

[26] Nathaniel J. Lindsey, Eileen R. Martin, Douglas S. Dreger, Barry Freifeld, Stephen Cole, Stephanie R. James, Biondo L. Biondi, and Jonathan B. Ajo-Franklin, Fiber-Optic Network Observations of Earthquake Wavefields, Geophys. Res. Lett. **44**, 11792 (2017).

[27] Nathaniel J. Lindsey, T. Craig Dawe, and Jonathan B. Ajo-Franklin, Illuminating seafloor faults and ocean dynamics with dark fiber distributed acoustic sensing, Science **366**, 1103 (2019).

[28] Kenji Numata, Amy Kemery, and Jordan Camp, Thermal-Noise Limit in the Frequency Stabilization of Lasers with Rigid Cavities, Phys. Rev. Lett. **93**, 250602 (2004).

[29] Seth M. Foreman, Kevin W. Holman, Darren D. Hudson, David J. Jones, and Jun Ye, Remote transfer of ultrastable frequency references via fiber networks, Rev. Sci. Instrum. **78**, 021101 (2007).

[30] S. Droste, F. Ozimek, Th. Udem, K. Predehl, T. W. Hänsch, H. Schnatz, G. Grosche, and R. Holzwarth, Optical-Frequency Transfer over a Single-Span 1840 km Fiber Link, Phys. Rev. Lett. **111**, 110801 (2013).

[31] C. Lisdat *et al.*, A clock network for geodesy and fundamental science, Nat. Commun. **7**, 12443 (2016).

[32] P. Delva *et al.*, Test of Special Relativity Using a Fiber Network of Optical Clocks, Phys. Rev. Lett. **118**, 221102 (2017).

[33] Giuseppe Marra, Cecilia Clivati, Richard Luckett, Anna Tampellini, Jochen Kronjäger, Louise Wright, Alberto Mura, Filippo Levi, Stephen Robinson, Andr Xuereb, Brian Baptie, and Davide Calonico, Ultrastable laser interferometry for earthquake detection with terrestrial and submarine cables, Science **361**, 486 (2018).

[34] Yaxi Yan, Hua Zheng, Alan Pak Tau Lau, Changjian Guo, and Chao Lu, Unidirectional ultra-long distributed optical fiber sensor, IEEE Photonics J. **13**, 1 (2021).

[35] See Supplemental Material at http://link.aps.org/supplemental/10.1103/PhysRevLett.128.180502 for detailed theoretical scheme, detailed experimental technologies, and full experimental results, which includes Refs. [36–40].

[36] Xiao-Long Hu, Cong Jiang, Zong-Wen Yu, and Xiang-Bin Wang, Sending-or-not-sending twin-field protocol for quantum key distribution with asymmetric source parameters, Phys. Rev. A **100**, 062337 (2019).

[37] Herman Chernoff, A measure of asymptotic efficiency for tests of a hypothesis based on the sum of observations, Ann. Math. Stat. **23**, 493 (1952).

[38] Alexander Vitanov, Frederic Dupuis, Marco Tomamichel, and Renato Renner, Chain rules for smooth min-and max-entropies, IEEE Trans. Inf. Theory **59**, 2603 (2013).

[39] Cong Jiang, Zong-Wen Yu, and Xiang-Bin Wang, Measurement-device-independent quantum key distribution with source state errors and statistical fluctuation, Phys. Rev. A **95**, 032325 (2017).

[40] Hongduo Zhao, Difei Wu, Mengyuan Zeng, and Sheng Zhong, A vibration-based vehicle classification system using distributed optical sensing technology, Transp. Res. Rec. **2672**, 12 (2018).

[41] Robert V. Pound, Electronic frequency stabilization of microwave oscillators, Rev. Sci. Instrum. **17**, 490 (1946).

[42] R. W. P. Drever, John L. Hall, F. V. Kowalski, J. Hough, G. M. Ford, A. J. Munley, and H. Ward, Laser phase and frequency stabilization using an optical resonator, Appl. Phys. B **31**, 97 (1983).

[43] Cong Jiang, Zong-Wen Yu, Xiao-Long Hu, and Xiang-Bin Wang, Unconditional Security of Sending or Not Sending Twin-Field Quantum Key Distribution with Finite Pulses, Phys. Rev. Applied **12**, 024061 (2019).

[44] Hai Xu, Zong-Wen Yu, Cong Jiang, Xiao-Long Hu, and Xiang-Bin Wang, Sending-or-not-sending twin-field quantum key distribution: Breaking the direct transmission key rate, Phys. Rev. A **101**, 042330 (2020).

[45] Cong Jiang, Xiao-Long Hu, Zong-Wen Yu, and Xiang-Bin Wang, Composable security for practical quantum key distribution with two way classical communication, New J. Phys. **23**, 063038 (2021).

[46] Cong Jiang, Xiao-Long Hu, Hai Xu, Zong-Wen Yu, and Xiang-Bin Wang, Zigzag approach to higher key rate of sending-or-not-sending twin field quantum key distribution with finite-key effects, New J. Phys. **22**, 053048 (2020).

[47] Juan Yin, Yu-Huai Li, Sheng-Kai Liao, Meng Yang, Yuan Cao, Liang Zhang, Ji-Gang Ren, Wen-Qi Cai, Wei-Yue Liu, Shuang-Lin Li *et al.*, Entanglement-based secure quantum cryptography over 1,120 kilometres, Nature (London) **582**, 501 (2020).